6-2013

Dispersive Waves in Microstructured Solids

A. Berezovski
Tallinn University of Technology

J. Engelbrecht
Tallinn University of Technology, je@ioc.ee

A. Salupere
Tallinn University of Technology

K. Tamm
Tallinn University of Technology

T. Peets
Tallinn University of Technology

See next page for additional authors

Dispersive waves in microstructured solids

A.Berezovski[a,*], J.Engelbrecht[a], A.Salupere[a], K.Tamm[a], T.Peets[a], M.Berezovski[b]

[a] *Centre for Nonlinear Studies, Institute of Cybernetics at Tallinn University of Technology, Akadeemia tee 21, 12618 Tallinn, Estonia*
[b] *Department of Mathematical Sciences, Worcester Polytechnic Institute, 100 Institute Rd, Worcester, MA, 01609, USA*

Abstract

The wave motion in micromorphic microstructured solids is studied. The mathematical model is based on ideas of Mindlin and governing equations are derived by making use of the Euler-Lagrange formalism. The same result is obtained by means of the internal variables approach. Actually such a model describes internal fields in microstructured solids under external loading and the interaction of these fields results in various physical effects. The emphasis of the paper is on dispersion analysis and wave profiles generated by initial or boundary conditions in a one-dimensional case.

Keywords: microstructured solids, wave propagation, dispersion

1. Introduction

Widely used materials in contemporary technological world like composites, functionally graded materials, polycrystalline solids, granular materials, etc., all have inherent microstructures at different scales. Additionally, high-frequency

*Corresponding author, Phone: +372 6204164, Fax: +372 6204151
Email address: Arkadi.Berezovski@cs.ioc.ee (A.Berezovski)

excitations are common in modern technology. In this case, wavelengths of excitations are comparable with internal scales in materials. Consequently, microstructural effects must be taken into account, especially when modeling and analyzing dynamical phenomena.

Microstructural effects are observed in wave propagation in solids when the wavelength of a travelling signal becomes comparable with the scale of material heterogeneities (Gonella, Greene and Liu, 2011). The influence of microstructure on wave propagation clearly manifests itself in the wave dispersion that alters both the shape and the velocity of propagating waves. Wave propagation in heterogeneous solids has been a subject of considerable research for many years. However, microstructural details are rarely taken into account in large-scale structural dynamics or dynamic impact simulations. The reason is the enormous complexity of wave phenomena in highly heterogeneous media.

There exist distinct approaches to the description of microstructural effects on wave propagation in solids. The first one is focused on the determining so-called effective properties of a material. It is expected that these averaged or smoothened properties reflect in some global sense the response of specimens of the material to external loads. Homogenization methods (Santosa and Symes, 1991; Chen and Fish, 2001; Fish and Fan, 2008) represent a pure mathematical asymptotic multiple-scale procedure under assumption of the validity of classical wave equation.

Another approach to model dispersion effects returns to the Born–von Kármán model for the one-dimensional atomic chain (Born and von Kármán, 1912). It

is the basis for derivation of higher-order dispersive wave equations by a continualization procedure (Metrikine and Askes, 2002; Fish et al., 2005; Askes et al., 2008; Andrianov et al., 2010, e.g.). Dispersive wave equations obtained by continualization and homogenization are discussed and unified by Berezovski et al. (2011).

A very straightforward approach to involve microstructural effects into the description of wave propagation is provided by higher order or generalized theories of elastic continua (Mindlin, 1964; Eringen and Suhubi, 1964). Generalized theories of continua extend conventional continuum mechanics by incorporating the micromotion into consideration. The micromorphic continuum description has enlarged the application area of continuum theory to the microscopic space and time scales (Wang and Lee, 2010). The well-established framework for higher grade and higher order theories is, however, accompanied by too many usually undetermined phenomenological coefficients.

The microcontinuum field theories are intended to provide a systematic extension of the continuum description of materials, some characteristic length scales of which are associated with their microstructure. We focus our attention on the micromorphic theory which is well suited to account for scale effects caused by the inherent microstructure (Forest, 2009). The basic model follows Mindlin (1964) who introduced material elements as cells able to deform independently of the main body. The governing equations are derived by making use of the Euler-Lagrange formalism (Engelbrecht et al., 2005).

The purpose of this paper is not to present a detailed overview on general-

ized theories of continua but to focus on the one-dimensional wave motion in microstructured solids based on mathematical models which in our view reflect best the main characteristics of physical effects in such solids. We would like to demonstrate that the description of wave motion in microstructured solids is improved by introducing internal fields due to internal variables combining continuum mechanics with thermodynamics. The main emphasis will be on the analyzes or in other words on "how does it work". The paper is actually a synthesis of recent studies which has been focused on wave motion in microstructured solids.

The paper is organized as follows. In Section 2, generic mathematical models for dispersive wave equations are discussed. Their structure depends on assumptions concerning the free energy. Several possible simplifications of governing equations are presented in Section 3, and feasible extensions are demonstrated in Section 4. Section 5 is devoted to the dispersion analysis of obtained models together with numerical solutions of typical initial and boundary value problems. These results are mostly based on research within graduate studies (Peets, 2011; Tamm, 2011) in order to synthesize a general view. Conclusions and final remarks are presented in the last Section.

2. Dispersive wave equation in one dimension

The structure of the dispersive wave equation is explicitly seen from the one-dimensional setting. Here we construct governing equations following first Mindlin (1964) and Engelbrecht et al. (2005) and then following the concept of

dual internal variables (Ván et al., 2008).

In the spirit of Mindlin (1964), we consider a continuum equipped by deformable cells characterized by the microdeformation φ. Note that in this simple one-dimensional case, φ is a scalar quantity. This additional degree of freedom together with the macrodisplacement u forms a quadratic potential energy W which can be specified as (Engelbrecht et al., 2005)

$$W = \frac{\rho_0 c^2}{2} u_x^2 + A\varphi u_x + \frac{1}{2} B\varphi^2 + \frac{1}{2} C\varphi_x^2, \tag{1}$$

where c is the longitudinal wave speed, and coefficients A, B, and C are material parameters characterizing microstructure influence. The Lagrangian $L = K - W$ can be constructed by intoducing the kinetic energy (Capriz, 1989)

$$K = \frac{\rho_0}{2} u_t^2 + \frac{I}{2} \varphi_t^2, \tag{2}$$

where I is the measure of microstructure inertia. It must be stressed that in the multi-dimensional case the microinertia tensor appears, which must be analyzed with care to avoid the incompatibility with the standard mechanics of rigid bodies (Mariano, 2008)).

By making use of Euler-Lagrange equations (for details, see (Engelbrecht et al., 2005)), the balance laws are obtained for macroscopic and microscopic scales

$$\rho_0 u_{tt} = \rho_0 c^2 u_{xx} + A\varphi_x, \tag{3}$$

$$I\varphi_{tt} = C\varphi_{xx} - Au_x - B\varphi. \tag{4}$$

Equations of motion (3) and (4) can be combined into a single dispersive wave

equation

$$u_{tt} = c^2 u_{xx} + \frac{C}{B}\left(u_{tt} - c^2 u_{xx}\right)_{xx} - \frac{I}{B}\left(u_{tt} - c^2 u_{xx}\right)_{tt} - \frac{A^2}{\rho_0 B} u_{xx}. \qquad (5)$$

For any particular material the parameters A, B, C, I should be specified as well as corresponding initial and boundary conditions for a given geometry and loading.

A slightly more general model for microstructure can be obtained by considering the microdeformation φ as an internal variable complemented by its dual counterpart ψ (an auxiliary internal variable). Following the concept of dual internal variables (Ván et al., 2008), we consider the free energy W as a general sufficiently regular function of the strain, temperature, two internal variables φ, ψ and their space derivatives

$$W = \overline{W}(u_x, \theta, \varphi, \varphi_x, \psi, \psi_x). \qquad (6)$$

In this case the equations of state define the macrostress σ, the entropy S, microstresses η and ζ, and interaction forces τ and ξ as follows:

$$\begin{gathered} \sigma := \frac{\partial \overline{W}}{\partial u_x}, \quad S := -\frac{\partial \overline{W}}{\partial \theta}, \quad \tau := -\frac{\partial \overline{W}}{\partial \varphi}, \quad \eta := -\frac{\partial \overline{W}}{\partial \varphi_x}, \\ \xi := -\frac{\partial \overline{W}}{\partial \psi}, \quad \zeta := -\frac{\partial \overline{W}}{\partial \psi_x}. \end{gathered} \qquad (7)$$

In the isothermal case the dissipation inequality reduces to the intrinsic part depending only on internal variables (Berezovski et al., 2009, 2011)

$$\Phi = (\tau - \eta_x)\varphi_t + (\xi - \zeta_x)\psi_t \geq 0. \qquad (8)$$

It is easy to see that the following choice of governing equations for internal variables

$$\varphi_t = R(\xi - \zeta_x), \qquad \psi_t = -R(\tau - \eta_x), \qquad (9)$$

where R is an appropriate constant, leads to zero dissipation. This means that dissipation inequality (8) is satisfied automatically with governing equations (9).

Keeping a quadratic free energy dependence in the form

$$\overline{W} = \frac{\rho_0 c^2}{2} u_x^2 + A u_x \varphi + A' u_x \varphi_x + \frac{1}{2} B \varphi^2 + \frac{1}{2} C \varphi_x^2 + \frac{1}{2} D \psi^2, \tag{10}$$

we see that the considered free energy function is the one-dimensional reduction of the general micromorphic strain energy density (Mindlin, 1964), where the product of the microdeformation φ and its gradient is replaced by the square of the second internal variable ψ. The corresponding macro- and microstresses follow from the equations of state

$$\sigma = \frac{\partial \overline{W}}{\partial u_x} = \rho_0 c^2 u_x + A\varphi + A'\varphi_x, \tag{11}$$

$$\eta = -\frac{\partial \overline{W}}{\partial \varphi_x} = -A' u_x - C\varphi_x, \tag{12}$$

as well as the interactive internal force

$$\tau = -\frac{\partial \overline{W}}{\partial \varphi} = -A u_x - B\varphi. \tag{13}$$

Accordingly, the balance of linear momentum results in

$$\rho_0 u_{tt} = \rho_0 c^2 u_{xx} + A\varphi_x + A'\varphi_{xx}, \tag{14}$$

and the governing equation for the primary internal variable φ has the form (Berezovski et al., 2011)

$$I\varphi_{tt} = C\varphi_{xx} + A' u_{xx} - A u_x - B\varphi, \tag{15}$$

if we use the same notation for the measure of microinertia as previosly. Here $I = 1/(R^2 D)$. It must be stressed that governing equation (15) follows from

dissipation inequality (8) by applying choice (9). Therefore, this approach is thermodynamically consistent.

The latter equations of motion can be combined in the single dispersive wave equation (Berezovski et al., 2011)

$$u_{tt} = c^2 u_{xx} + \frac{C}{B}\left(u_{tt} - c^2 u_{xx}\right)_{xx} - \frac{I}{B}\left(u_{tt} - c^2 u_{xx}\right)_{tt} + \frac{A'^2}{\rho_0 B} u_{xxxx} - \frac{A^2}{\rho_0 B} u_{xx}. \tag{16}$$

Dispersive wave equation (16) is sufficiently general to cover all existing one-dimensional microstructure models (Berezovski et al., 2011). In fact, with $A = 0$ it is equivalent to "causal" model by Metrikine (2006), while with $A' = 0$ it is reduced to the Mindlin-type model by Engelbrecht et al. (2005) (cf. Eq. 5). The Maxwell-Rayleigh model of anomalous dispersion (Maugin, 1995) corresponds to the choice $A = 0, A' = 0$, and $C = 0$, and more classical linear version of the Boussinesq equation for elastic crystals and the Love-Rayleigh equation for rods accounting for lateral inertia (cf. Maugin (1995)) can be obtained choosing $A = 0, I = 0, C = 0$ and $A = 0, I = 0, \rho c^2 C = A'^2$, respectively.

Dispersive wave equation (16) can be also represented in terms of distinct wave operators

$$u_{tt} - \left(c^2 - \frac{A^2}{\rho_0 B}\right) u_{xx} = \frac{C}{B}\left(u_{tt} - \left(c^2 - \frac{A'^2}{\rho_0 C}\right) u_{xx}\right)_{xx} - \frac{I}{B}\left(u_{tt} - c^2 u_{xx}\right)_{tt}. \tag{17}$$

Introducing the wave speed related to the microstructure

$$c_1^2 = \frac{C}{I}, \tag{18}$$

we can identify corrections to wave velocity due to couplings as follows:

$$c_A^2 = \frac{A^2}{\rho_0 B}, \quad c_{A'}^4 = \frac{A'^2}{\rho_0 I}, \tag{19}$$

and represent dispersive wave equation (17) as

$$u_{tt} - \left(c^2 - c_A^2\right) u_{xx} = p^2 c_1^2 \left(u_{tt} - \left(c^2 - \frac{c_{A'}^4}{c_1^2}\right) u_{xx}\right)_{xx} - p^2 \left(u_{tt} - c^2 u_{xx}\right)_{tt}, \tag{20}$$

with $p^2 = I/B$. All three wave operators in Eq. (20) are different and reflect characteristics of macro- and microstructure and their coupling.

As one can see, Mindlin-type dispersive wave equation (5) and unified dispersive wave equation (16) differ from each other only by the single term containing the fourth-order space derivative. This leads, however, to three distinct wave operators in Eq. (20) instead of two of them in Eq. (5).

Unified dispersive wave equation (16) and/or Mindlin-type dispersive wave equation (5) are basic material models for the analysis of 1D problems including further simplification (Section 3) or extension (Section 4). As far as the classical wave equation is considered as the cornerstone for wave dynamics of homogeneous media, these models allow to demonstrate specific dispersion effects which are characteristic to microstructured materials.

3. Model simplifications

3.1. Reduction by the slaving principle

Governing equations (16) or (20) include several wave operators which describe the motion in macro- and microscale. It is possible to distinguish leading operators by using the slaving principle (Porubov, 2003). By means of series

representation and the slaving principle (for details, see (Engelbrecht et al., 2005)) we get finally

$$u_{tt} - \left(c^2 - c_A^2\right) u_{xx} = p^2 c_A^2 \left(u_{tt} - c_1^2 u_{xx}\right)_{xx} . \tag{21}$$

Equation (21) reflects clearly the hierarchical character of wave propagation in microstructured materials following Whitham (1974). Indeed:

(i) if pc_A is small then the terms in the r.h.s. are negligible; if $p\,c_A$ is large then, vice versa, the terms in the l.h.s. are negligible and the wave characteristics are governed by properties of microstructure;

(ii) the wave speed in the compound material is affected by the microstructure (c^2 versus $c^2 - c_A^2$) and only $A = 0$ (no coupling) excludes this dependence;

(iii) the influence of the microstructure is, as expected, characterized by dispersive terms of the fourth-order (u_{ttxx} and u_{xxxx}).

The nonlinear governing equations will be presented in Section 4.3. The comparison of model equations (16) and (21) will be given in Section 5.2.

3.2. One-wave asymptotics

The model equation derived in Section 2.1. actually generalizes the classical wave equation which describe two waves – one propagating to the right, another – to the left. There exist powerful methods which allow to derive so-called evolution equations describing just the propagation of one wave along the chosen characteristics. These asymptotic (reductive perturbation) methods are described in details, for example by Engelbrecht (1983). Applying the reductive perturbation method for Eq. (5) the following evolution equation is derived

(Peets et al., 2008; Randrüüt et al., 2009):

$$v_T + \frac{c_A^2 - c_1^2}{c_A^2} v_{XXX} = 0, \tag{22}$$

where $v = U_X$, $U(X,T) = u/l$, $X = (x - c_A t)/L$, $T = c_A l t/2L^2$, and L and l are macroscale and microscale, respectively.

Equation (22) is the linearized Korteweg-de Vries (KdV) equation. If the reductive perturbation method is applied for the hierarchical equation (21) then the result will be the same Eq. (22). This means that basic Eq. (16) and its asymptotic (hierarchical) approximation (21) yield the evolution equation in the same form. The case of nonlinear models will be dealt in Section 4.3.

4. Model extensions

Microstructure model (14)–(15) allows not only the reduction, but also the extension in various directions. The most desired extensions regard to several microstructures and to nonlinear effects.

4.1. Double microstructure

The extension of microstructure model (14)–(15) to the case with two microstructures can be achieved in different ways. The first one is the "hierarchy of microstructures"(Engelbrecht et al., 2006). In this case, the coupling of the corresponding microstructure hierarchy may be represented schematically as follows (Fig. 1).

This means that only the motion of the first microstructure is coupled with the macromotion, and the motion of the second microstructure is coupled with

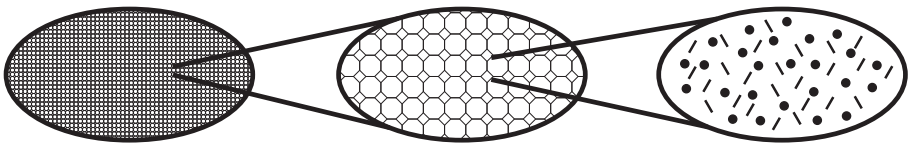

Figure 1: Hierarchical microstructures.

that of the first one. In this case, the free energy is dependent on two internal variables φ_1 and φ_2 as follows:

$$\begin{aligned} W = \frac{\rho_0 c^2}{2} u_x^2 + A_1 \varphi_1 u_x + \frac{1}{2} B_1 \varphi_1^2 + \frac{1}{2} C_1 (\varphi_1)_x^2 + \\ + A_{12} (\varphi_1)_x \varphi_2 + \frac{1}{2} B_2 \varphi_2^2 + \frac{1}{2} C_2 (\varphi_2)_x^2. \end{aligned} \tag{23}$$

This leads to expressions of stresses in the form

$$\begin{aligned} \sigma = \frac{\partial W}{\partial u_x} = \rho_0 c^2 u_x + A_1 \varphi_1, \\ \eta_1 = -\frac{\partial W}{\partial (\varphi_1)_x} = - C_1 (\varphi_1)_x - A_{12} \varphi_2, \quad \eta_2 = -\frac{\partial W}{\partial (\varphi_2)_x} = -C_2 (\varphi_2)_x, \end{aligned} \tag{24}$$

and to interactive internal forces

$$\tau_1 = -\frac{\partial W}{\partial \varphi_1} = -A_1 u_x - B_1 \varphi_1, \quad \tau_2 = -\frac{\partial W}{\partial \varphi_2} = -A_{12} (\varphi_1)_x - B_2 \varphi_2. \tag{25}$$

Accordingly, equations of motion take the form

$$\rho_0 u_{tt} = \sigma_x = \rho_0 c^2 u_{xx} + A_1 (\varphi_1)_x, \tag{26}$$

$$I_1 (\varphi_1)_{tt} = \tau_1 - (\eta_1)_x = C_1 (\varphi_1)_{xx} - A_1 u_x - B_1 \varphi_1 + A_{12} (\varphi_2)_x, \tag{27}$$

$$I_2 (\varphi_2)_{tt} = \tau_2 - (\eta_2)_x = C_2 (\varphi_2)_{xx} - A_{12} (\varphi_1)_x - B_2 \varphi_2, \tag{28}$$

where I_1 and I_2 are appropriate internal inertia measures. The very same model is presented by Pastrone (2010) including nonlinear terms at the macroscopic level.

Another example of possible coupling of macromotion and microstructures can be constructed by means of the representation of the free energy dependence as the sum of two similar contributions (cf. (Berezovski et al., 2010))

$$W = \frac{\rho_0 c^2}{2} u_x^2 + A_1 \varphi_1 u_x + A_1' (\varphi_1)_x u_x + \frac{1}{2} B_1 \varphi_1^2 + \frac{1}{2} C_1 (\varphi_1)_x^2 + \frac{1}{2} D_1 \psi_1^2 + \\ + A_2 \varphi_2 u_x + A_2' (\varphi_2)_x u_x + \frac{1}{2} B_2 \varphi_2^2 + \frac{1}{2} C_2 (\varphi_2)_x^2 + \frac{1}{2} D_2 \psi_2^2, \tag{29}$$

where ψ_1 and ψ_2 are auxiliary internal variables (cf. Eq. (10)). In the considered case, both equations of motion for microstructures are coupled with the balance of linear momentum for the macromotion, but not coupled with each other. This is illustrated in Fig. 2.

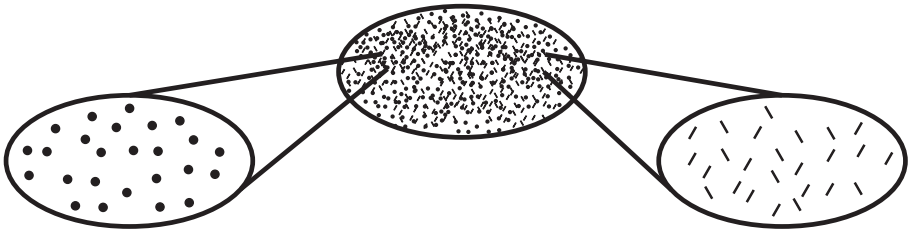

Figure 2: Concurrent microstructures.

Corresponding stresses are determined as follows:

$$\sigma = \frac{\partial W}{\partial u_x} = \rho_0 c^2 u_x + A_1 \varphi_1 + A_2 \varphi_2 + A_1' (\varphi_1)_x + A_2' (\varphi_2)_x, \tag{30}$$

$$\eta_1 = -\frac{\partial W}{\partial (\varphi_1)_x} = -A_1' u_x - C(\varphi_1)_x, \quad \zeta_1 = -\frac{\partial W}{\partial (\psi_1)_x} = 0, \tag{31}$$

$$\eta_2 = -\frac{\partial W}{\partial (\varphi_2)_x} = -A_2' u_x - C(\varphi_2)_x, \quad \zeta_2 = -\frac{\partial W}{\partial (\psi_2)_x} = 0, \tag{32}$$

as well as interactive internal forces:

$$\tau_1 = -\frac{\partial W}{\partial \varphi_1} = -A_1 u_x - B_1 \varphi_1, \quad \tau_2 = -\frac{\partial W}{\partial \varphi_2} = -A_2 u_x - B_2 \varphi_2. \tag{33}$$

Accordingly, equations of motion take the form

$$\rho_0 u_{tt} = \rho_0 c^2 u_{xx} + A_1(\varphi_1)_x + A_2(\varphi_2)_x + A_1'(\varphi_1)_{xx} + A_2'(\varphi_2)_{xx}, \tag{34}$$

$$I_1(\varphi_1)_{tt} = C_1(\varphi_1)_{xx} + A_1' u_{xx} - A_1 u_x - B_1\varphi_1, \tag{35}$$

$$I_2(\varphi_2)_{tt} = C_2(\varphi_2)_{xx} + A_2' u_{xx} - A_2 u_x - B_2\varphi_2. \tag{36}$$

The doubling of the number of coefficients in the double microstructure model in comparison to the single microstructure complicates the quantitative analysis of the model. Nevertheless, it can be qualitatively analyzed by studying dispersion curves (see Section 5.1.2).

4.2. Nonlinearities

In Section 2, the free energy W was determined with the accuracy of quadratic terms (see expressions (1) and (10)). In order to model physical nonlinearities, cubic terms should also be taken into account. Then instead of Eq. (1) we have to consider a more general free energy function

$$W = \frac{\rho_0 c^2}{2} u_x^2 + A\varphi u_x + \frac{1}{2} B\varphi^2 + \frac{1}{2} C\varphi_x^2 + \frac{1}{6} N u_x^3 + \frac{1}{6} M\varphi_x^3, \tag{37}$$

where terms with coefficients N and M are responsible for the nonlinearity in the macro- and microscale, respectively. Then system of equations (3) and (4) is transformed to

$$\rho_0 u_{tt} = \rho_0 c^2 u_{xx} + A\varphi_x + N u_x u_{xx}, \tag{38}$$

$$I\varphi_{tt} = C\varphi_{xx} - A u_x - B\varphi + M\varphi_x\varphi_{xx}. \tag{39}$$

By using the asymptotic procedure like it was done for deriving Eq. (20), here system of Eqs. (38), (39) yields (for details see (Engelbrecht et al., 2006))

$$u_{tt} - \left(c^2 - c_A^2\right) u_{xx} - \frac{\mu}{2}\left(u_x^2\right)_x = p^2 c_A^2 \left(u_{tt} - c_1^2 u_{xx}\right)_{xx} + \frac{\lambda}{2}\left(u_{xx}^2\right)_{xx}. \qquad (40)$$

where μ and λ are combinations of material and geometrical parameters. Alternatively, Eq. (40) can be written in terms of deformation $v = u_x$

$$v_{tt} - \left(c^2 - c_A^2\right) v_{xx} - \frac{\mu}{2}\left(v^2\right)_x = p^2 c_A^2 \left(v_{tt} - c_1^2 v_{xx}\right)_{xx} + \frac{\lambda}{2}\left(v_x^2\right)_{xxx}. \qquad (41)$$

Both Eqs. (40) and (41) belong to the family of Boussinesq-type equations (Christov et al. (2007), Engelbrecht et al. (2011)). Comparing Eqs. (40) and (41) with Eq. (20), it is clear that in the latter case the wave operators are nonlinear and reflect the influence of nonlinearities in macro- and microlevel. The corresponding nonlinear evolution equation derived on the basis of slaving principle is the following (Randrüüt et al., 2009):

$$v_T + \frac{c_N^2}{2c_A^2}(v^2)_X + \frac{c_A^2 - c_1^2}{c_A^2} v_{XXX} + \frac{l c_M^2}{2L c_A^2}(v_X^2)_{XX} = 0, \qquad (42)$$

where

$$c_N^2 = \frac{N}{\rho}, \quad c_M^2 = \frac{MA}{IBL}. \qquad (43)$$

This is a modified KdV equation with two nonlinear terms: (i) the second term in l.h.s of Eq. (42) reflects the nonlinearity in the macroscale; (ii) the fourth term reflects the nonlinearity in the microscale. If $c_M = 0$ then Eq. (42) reduces to the classical KdV equation. It is certainly possible to transform Eq. (42) into the standardized form (Randrüüt and Braun, 2010)

$$q_t + 6qq_x + q_{xxx} + 3k(q_x^2)_{xx} = 0 \qquad (44)$$

after suitable transformation of dependent and independent variables. Note that here q is related to deformation v.

5. Dispersion analysis

5.1. Dispersion relations

5.1.1. Single microstructure

The presence of higher-order derivatives in Eqs. (20) and (21) indicates the influence of dispersion. Dispersion relations can be derived by assuming the solution in the form of harmonic waves

$$u(x,t) = \hat{u}e^{i(kx-\omega t)}, \tag{45}$$

with the wave number k, the frequency ω, and the amplitude $\hat{u}$.

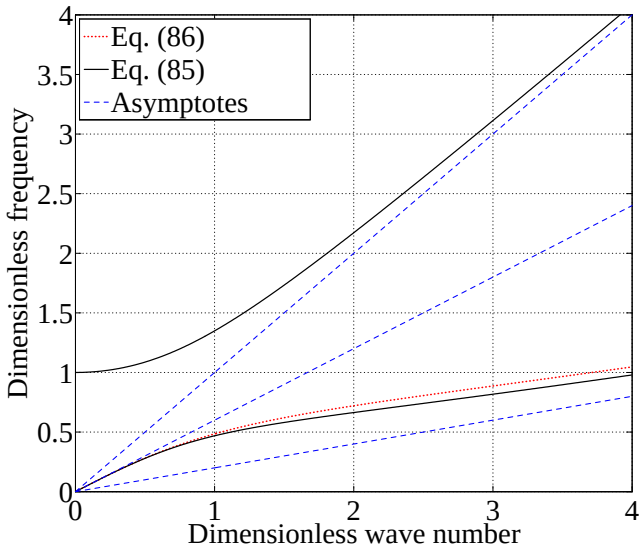

Figure 3: Dispersion curves in case of $c_{gr} < c_{ph}$ ($c_A = 0.8c, c_1 = 0.2c$).

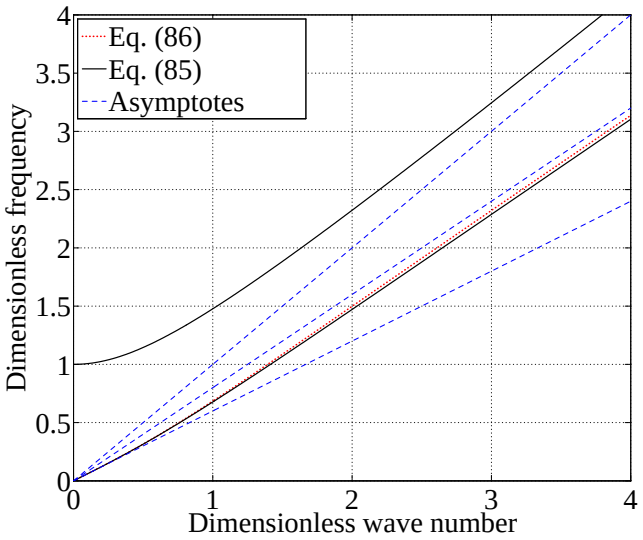

Figure 4: Dispersion curves in case of $c_{gr} > c_{ph}$ ($c_A = 0.8c, c_1 = 0.8c$).

Introducing expression (45) into Eqs. (20) and (21), we obtain

$$\omega^2 = \left(c^2 - c_A^2\right) k^2 + p^2 \left(\omega^2 - c^2 k^2\right) \left(\omega^2 - c_1^2 k^2\right), \tag{46}$$

$$\omega^2 = \left(c^2 - c_A^2\right) k^2 - p^2 c_A^2 \left(\omega^2 - c_1^2 k^2\right) k^2, \tag{47}$$

respectively. In order to simplify our discussion, we assume $A' = 0$.

Preliminary analysis shows immediately that in the long wave limit ($pck \ll 1$) both dispersion relations (46) and (47) provide the same limiting speed $c_R = (c^2 - c_A^2)^{1/2}$, which means that wave propagation in the medium with microstructure is slower than in the case without microstructure (Peets et al., 2008). This is direct consequence of the inclusion of the microstructure (Mindlin, 1964). In the short wave limit ($pck \gg 1$) full dispersion relation (46) provides two modes of wave propagation – one with the speed c_1 characteristic to the

microstructure and the other with the elastic wave speed c of the medium without microstructure. As hierarchical model (47) is an approximated one, in the short wave limit only the speed c_1 appears in this model.

The typical dispersion curves are shown in Figs. 3 and 4. Dispersion relation (46) which corresponds to full Eq. (20) is represented by solid lines and consists of two branches – acoustic (lower branch) and optical (upper branch). Dispersion relation (47) which corresponds to approximated Eq. (21) is represented by dotted lines while dashed lines correspond to asymptotic lines $\omega = k, \omega = c_1 k/c, \omega = c_R k/c$.

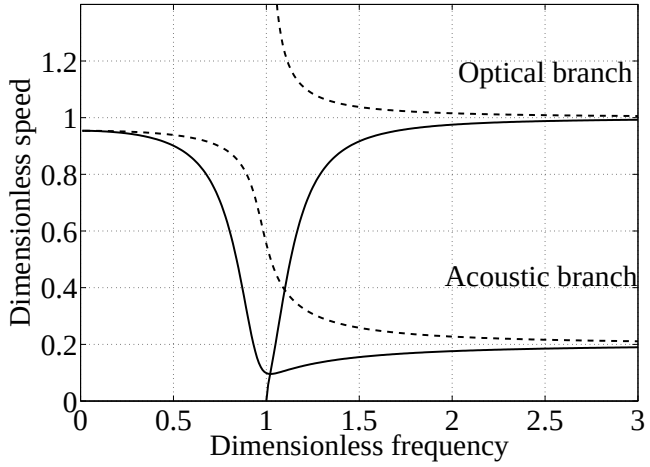

Figure 5: Group (solid line) and phase (dashed line) speed curves against the frequency, $c_A = 0.3c, c_1 = 0.2c$.

In general, the dispersion type following the acoustic dispersion branch can be either normal ($c_{gr} < c_{ph}$, see Fig. 3) or anomalous ($c_{gr} > c_{ph}$, see Fig. 4). Here c_{gr} and c_{ph} denote group and phase speed, respectively. The dispersion

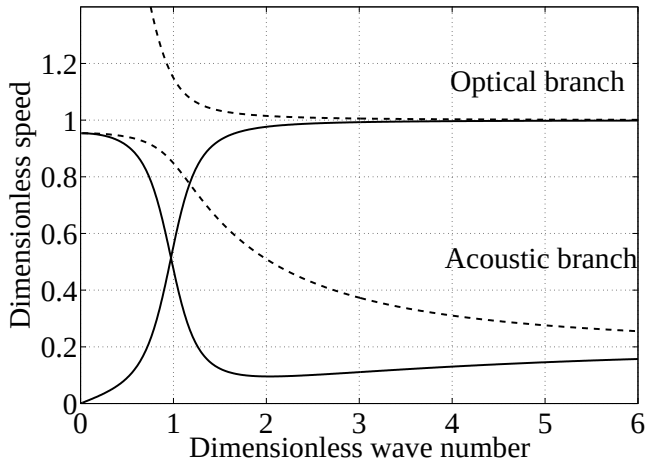

Figure 6: Group (solid line) and phase (dashed line) speed curves against the wave number, $c_A = 0.3c, c_1 = 0.2c$.

type of the optical branch in our case is always normal. The phase speed ($c_{ph} = \omega/k$) and the group speed ($c_{gr} = \partial\omega/\partial k$) reveal dispersion effects even more explicitly.

The phase and group speeds are depicted in Fig. 5 (against the frequency) and in Fig. 6 (against the wave number). While the asymptotic value of acoustic phase speed curve approaches gradually the value c_1/c, the group speed curve changes faster, initially assuming the value that is lower than c_1/c and then approaching this value. In the case of very strong normal dispersion (i.e. $c_R \gg c_1$), the group velocity curve assumes a value that is very close to zero before approaching the asymptotic value c_1/c. the effect becomes more subtle when $c_R \approx c_1$.

It is interesting to compare the accuracy of dispersion relation (47) which

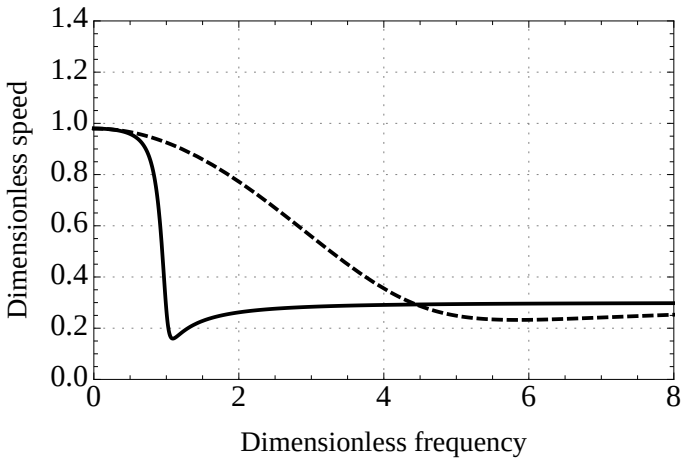

Figure 7: Behaviour of the group speed curves for Eqs. (20) (solid line) and (21) (dashed line) against the frequency, $c_A = 0.2c, c_1 = 0.3c$.

corresponds to hierarchical approximation (21) against dispersion relation (46) which corresponds to full equation (20). In some cases the difference could be rather large like in the case shown in Fig. 7. Obviously, the differences depend on material properties. Peets et al. (2008) have shown that in this context the main parameters are velocity ratios c_A/c and c_1/c.

The ranges of parameters are shown in Fig. 8 where values of speeds obtained from both relations agree within 5% error (the area between dashed lines) and within 10% error (the area between solid lines) at $k = 1.5/pc$. The behaviour for higher values of k is similar; only the area of good agreement becomes narrower. When k becomes very large, the area of good agreement becomes larger (Peets et al., 2008).

The physical situation studied above is similar to cases analysed by Papargyri-Beskou et al. (2009) who also have included microstructural and micro-inertial

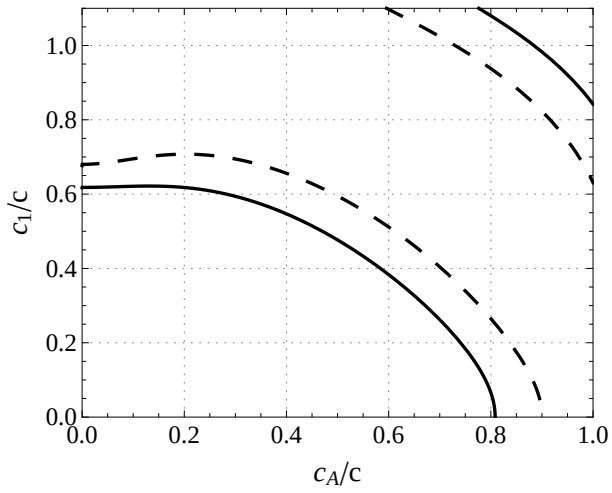

Figure 8: The accuracy of the approximation (21).

terms into governing equations. Here, however, the clear analysis of both branches of dispersion curves gives more insight to the understanding of the importance of micro-inertial terms (see also (Wang and Sun, 2002)).

5.1.2. Double microstructure

In case of hierarchical (Eqs. (26)–(28)) and concurrent (Eqs. (34)–(36)) microstructures the dispersion relations are certainly more complicated. Instead of relation (46) we get the following

$$\begin{aligned}&(c^2k^2-\omega^2)(c_1^2k^2-\omega^2+\omega_1^2)(c_2^2k^2-\omega^2+\omega_2^2)-\\&-c_{A12}^2\omega_2^2k^2(c^2k^2-\omega^2)-c_{A1}^2\omega_1^2k^2(c_2^2k^2-\omega^2+\omega_2^2)=0,\end{aligned}\tag{48}$$

$$\begin{aligned}&(c^2k^2-\omega^2)(c_1^2k^2-\omega^2+\omega_1^2)(c_2^2k^2-\omega^2+\omega_2^2)+\\&+c_{A2}^2\omega_2^2k^2(c_1^2k^2-\omega^2+\omega_1^2)-c_{A1}^2\omega_1^2k^2(c_2^2k^2-\omega^2+\omega_2^2)=0,\end{aligned}\tag{49}$$

respectively, for the hierarchical and concurrent models.

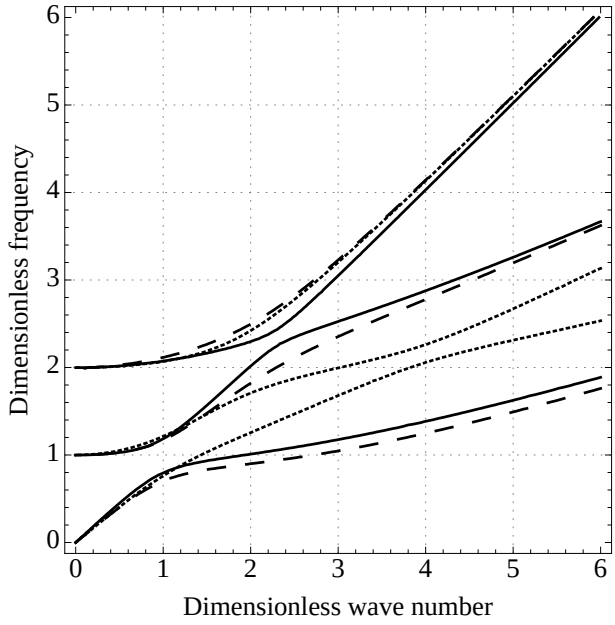

Figure 9: Comparison of dispersion curves of Eqs. (48) – solid lines, (49) – dashed lines, (51) – dotted lines. Here $c_{A1} = c_{A2} = c_{A12} = 0.4c, c_1 = 0.5c, c_1 = 0.3c$.

Here parameters

$$c_1^2 = \frac{C_1}{I_1}, \quad c_2^2 = \frac{C_2}{I_2}, \quad c_{A1}^2 = \frac{A_1^2}{\rho_0 B_1}, \quad c_{A2}^2 = \frac{A_2^2}{\rho_0 B_2}, \quad \omega_1^2 = \frac{B_1}{I_1}, \quad \omega_2^2 = \frac{B_2}{I_2}, \tag{50}$$

have been introduced.

In addition, it is possible that two concurrent microstructures which are described by free energy function (29) influence also each other. Then free energy function (29) should be enlarged by a term $A_{12}\varphi_{1x}\varphi_2$ – cf. free energy function (23). Then the dispersion relation reads

$$\begin{aligned}(c^2k^2 - \omega^2)(c_1^2k^2 - \omega^2 + \omega_1^2)(c_2^2k^2 - \omega^2 + \omega_2^2) + c_{A12}^2\omega_2^2k^2(-c_0^2k^2 + \omega^2) - \\ - c_{A1}^2\omega_1^2k^2(c_2^2k^2 - \omega^2 + \omega_2^2) - c_{A2}^2k^2\omega_2^2(c_1^2k^2 - \omega^2 + \omega_1^2) = 0,\end{aligned} \tag{51}$$

with $c_{A12}^2 = A_{12}^2/I_1 B_2$.

Dispersion curves for all cases (48), (49), and (51) are shown in Fig. 9. We limit ourselves to the case with $\omega_1 = 1, \omega_2 = 2, c_1/c > c_2/c$. It is seen immediately that while the behaviour of hierarchical model (48) and concurrent model (49) is quite similar, concurrent model with coupled microstructures (51) departs drastically from others in the region of medium-range wavelengths. It can therefore be concluded that the coupling between the microstructures has a significant effect on the dispersion in that region. The detailed analysis of all features of dispersion curves is presented by Peets (2011).

The models analysed above describe the physical situation clearly on the basis of the interaction of physical constituents (see Section 3). If the micro-displacement is described by a series representation (Huang and Sun, 2008) then dispersion curves have also several branches like in Fig. 9, but in this context correction factors are needed to adjust phase velocities of higher wave modes.

5.2. Wave profile analysis

The numerical simulation for boundary and initial value problems demonstrates clearly the influence of dispersion effects on wave profiles (Tamm, 2011; Peets, 2011). Here we show only a couple of typical cases.

(i) linear case, sinusoidal boundary conditions for system of equations (14), (15) with $A' = 0$. The frequency of the boundary excitation is limited to the range where only acoustic dispersion exists (dimensionless frequency is less than 1, see Fig. 10a), although due to coupling effects in the course of propagation

the influence of the optical branch can be seen.

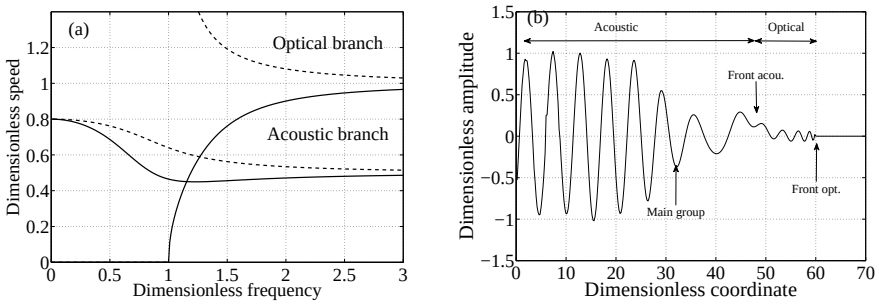

Figure 10: (a) - phase (dotted lines) and group (solid lines) speed curves and (b) wave profile at 60 time steps. Here $c_A = 0.6c, c_1 = 0.5c$, dimensionless frequency for the boundary condition is equal 0.8.

The Laplace transform technique is used with the inverse transform accomplished numerically (for details see Peets (2011)). A typical wave profile is shown in Fig. 10b. This wave profile can roughly be divided into two parts – high amplitude acoustic one and low amplitude optical part. Points denoted as "front acoustic" and "front optical" are related to maximal asymptotic speeds derived from the acoustic and optical dispersion curves, respectively. Point denoted as "main group" is related to the group speed of the dimensionless frequency 0.8 which is the frequency of the harmonic boundary condition.

For convenience we also divide the acoustic part into the main part, which has the amplitude almost equal to unity (the wave profile up to the point "main group"), and the medium amplitude part (the wave profile between the points "main group" and "front acoustic").

The main acoustic part travels at the group speed $0.53c$ corresponding to

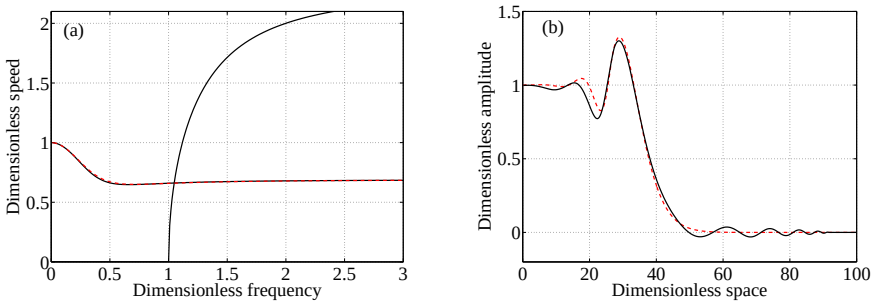

Figure 11: Group speed curves (a) and wave profiles for Heaviside-type boundary conditions at 40 time steps (b). Solid line - Eq. (20), dashed line - Eq. (21). Here $c_A = 0.9c, c_1 = 0.3c$.

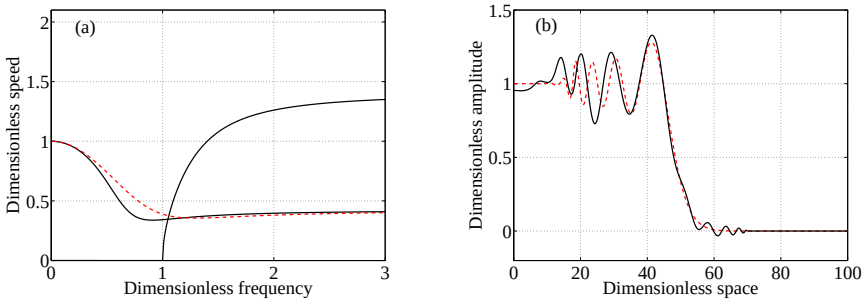

Figure 12: Group speed curves (a) and wave profiles for Heaviside-type boundary conditions at 50 time steps (b). Solid line - Eq. (20), dashed line - Eq. (21). Here $c_A = 0.7c, c_1 = 0.3c$.

the dimensionless frequency 0.8 at given material parameters (Fig. 10a). The approximate dimensionless wavelength can be estimated from Fig. 10b by measuring the distance between the two adjacent wave crests. The measured dimensionless wavelength for main acoustic part 5.40 is in good agreement with the dimensionless wave length 5.44 given by the dispersion analysis. The medium amplitude acoustic part travels at the group speed $0.8c$ which corresponds to the highest asymptotic value of the acoustic dispersion branch (Fig. 10a). As at the given frequency there are differences in phase and group speeds, the medium

amplitude part is slightly out of phase (Fig. 10b).

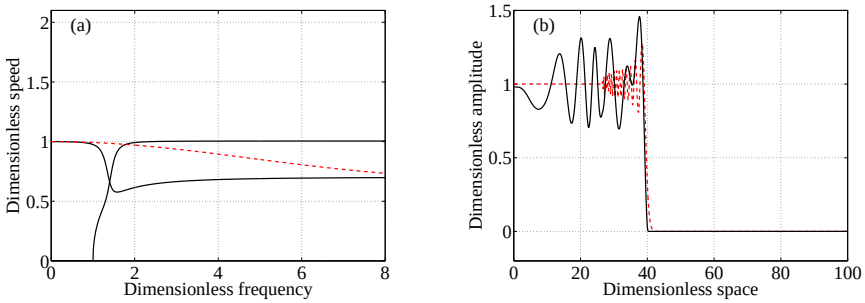

Figure 13: Group speed curves (a) and wave profiles for Heaviside-type boundary conditions at 40 time steps (b). Solid line - Eq. (20), dashed line - Eq. (21). Here $c_A = 0.1c, c_1 = 0.7c$.

The optical part of the wave profile is a low amplitude part that travels at the asymptotic speed of the optical dispersion branch which is equal to unity. This high frequency and low amplitude optical part reflects the effect of the optical dispersion branch. The amplitude of the optical part depends on the frequency of the boundary excitation.

(ii) linear case, Heaviside-type boundary conditions with $A' = 0$ for full equation (20) and its hierarchical approximation (21). The solutions are obtained in the similar way to the case (i). Typical wave profiles are shown in Figs. 11 – 13.

It can be seen that regardless of the differences in wave profiles, hierarchical model (21) provides good approximation of full model (20) (see Figs. 11 and 12). However the wave profile corresponding to Eq. (21) departs from full model (20) when $c_A/c \to 0$ (Fig. 13). The low amplitude oscillations in front of the main pulse in Figs. 11 and 12 reflect the influence of the optical dispersion

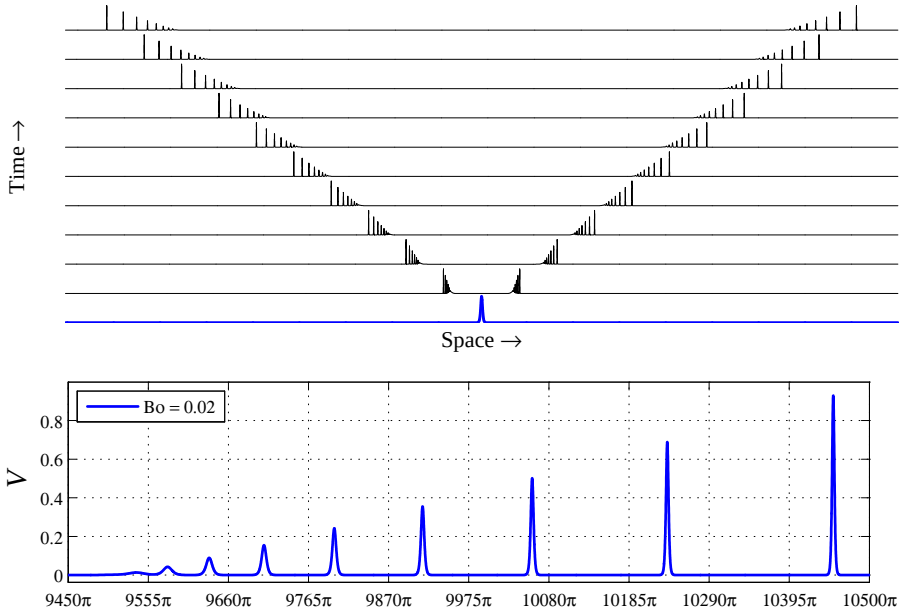

Figure 14: Formation of train of solitons for $B_0 = 0.02, K = 5500$, profiles plotted at every 1500 time steps.

branch.

(iii) nonlinear case, sech^2-type initial conditions for hierarchical equation (41). The solution is obtained by the pseudospectral method (Salupere, 2009; Tamm, 2011). The presence of both nonlinearities and dispersion in Eq. (41) indicates to the possibility of emergence of solitary waves. While the classical soliton equations (like KdV equation) are of the one-wave equations, Eq. (41) is of the Boussinesq-type (Christov et al., 2007; Engelbrecht et al., 2011) and describes the waves propagating to the right and to the left. Starting from the localized initial conditions

$$v(x,0) = v_0 \mathrm{sech}^2 B_0(x - x_0), \tag{52}$$

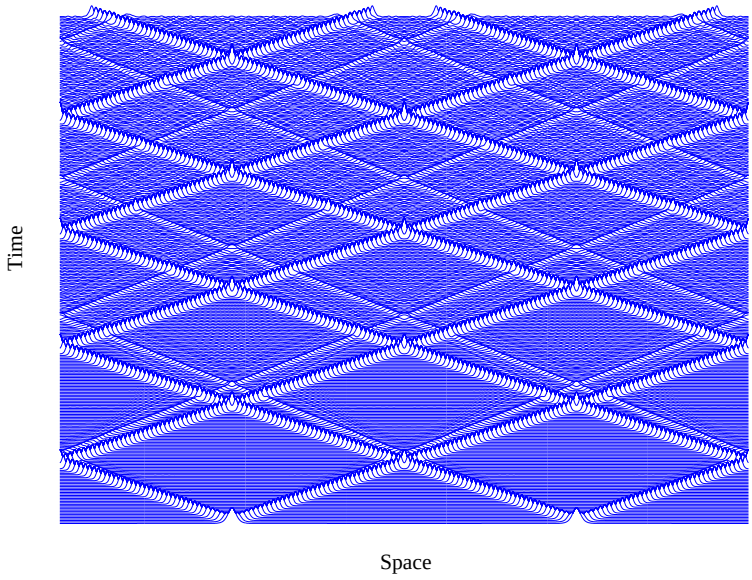

Figure 15: Interaction of solitons – time-slice plot.

where v_0 is the amplitude of initial excitation and parameter B_0 is related to the width of the initial pulse and using periodic boundary conditions

$$v(x,t) = v(x + 2Kk\pi, t), \tag{53}$$

where K is the number of 2π periods within a space domain and $k = 1, 2, \ldots$ the emerging soliton trains are shown in Fig. 14 (cf. Engelbrecht et al. (2011)).

Indeed in this case two trains of solitons emerge propagating to the right and to the left. To the best of the authors' knowledge, such a description was shown first by Engelbrecht et al. (2011) within the same model but with different parameters resulting in different trains.

(iv) interactions of solitons. According to the classical definition of solitons, every soliton should restore its amplitude (and speed) after interaction with

other solitons. While the KdV-type equation permits to model only the process of overtaking of solitons, here the Boussinesq-type model permits also to analyse the head-on collision. First, it must be stressed that due to the nonlinearity at the microscale, the emerging solitons are asymmetric. This is shown by numerical calculations (Tamm, 2011) and also by the analysis of Eq. (44) – see Randrüüt and Braun (2010). The numerical calculations demonstrate that the interaction of solitons is not fully elastic (Fig. 15).

The presence of radiation is clearly seen and that is why the notion of solitons in this case can be used only conditionally. This is also demonstrated by Khusnutdinova et al. (2009) in the case of models derived from lattice dynamics. On the other hand, however, it is known that single solitary waves modeled by Eq. (41) exist (Janno and Engelbrecht, 2005). The interaction of solitary waves are of importance in many Boussinesq-type systems (Christov et al., 2007; Maugin, 2011). However, a more detailed analysis of interaction processes is needed like it is done for KdV-type (one-wave) systems.

6. Final remarks

The aim of the paper was to analyse the structure and properties of the micromorphic-type microstructure model for describing the wave motion. As described above, the model reflects the influence of the internal structure on the macromotion of solids in a sufficiently general way. Actually this model describes internal fields in solids under external loading and the interaction of these fields results in various physical effects.

Main results described in this paper can be formulated as follows:

- The resulting microstructure model depends on the form of the free energy dependence. The dispersive wave equation can be represented in terms of distinct wave operators (20) describing the motion of macro- and microstructure. The scale parameters govern the wave motion indicating the relative strength of one wave operator or another (Engelbrecht et al., 2006). Approximation (21) is an excellent example of a simple hierarchical structure of wave operators in Whitham's sense (Whitham, 1974), while dispersive wave equation (20) has a mixed type of hierarchy which depends on rates of change in time or in space.

- The coupling between macro- and micromotion is governed by the corresponding mixed product terms in the free energy function. The influence of the coupling manifests itself not only in dispersion effects, but also in the changes of macroscopic velocity. This effect is demonstrated also by numerical simulation of 2D wave propagation (Engelbrecht et al., 2005).

- If physical nonlinearities are included into the free energy function, then the resulting governing wave equation is of the Boussinesq type. The numerical solution of this two-wave equation demonstrates the emergence of soliton trains propagating in 1D case to the right and to the left (Tamm, 2011). The one-wave approximation results in an evolution equation which belongs to the KdV-family (Randrüüt and Braun, 2010). Their soliton-type solutions exhibit asymmetry caused by the nonlinearities on the mi-

croscale.

- The generalization of the microstructure model on the multiscale case (Berezovski et al., 2010; Peets, 2011) is natural either for hierarchical microstructures or for concurrent microstructures. The resulting dispersive wave equation includes sixth order terms. In contrast to models derived from lattice dynamics, the higher order terms always form the corresponding wave operators (Engelbrecht et al., 2006).

- The specific features of group speed changes against frequencies are clearly reflected in changes of wave profiles. Precursors of main wave travel faster than the main pulse and their speed is determined by the properties of the optical branches of dispersion curves (Peets, 2011).

- The physical parameters of materials used for deriving the governing equations must be determined for applications. For models described in this paper, Janno and Engelbrecht (2011) have proposed several algorithms on the basis of direct measurements of phase and group velocities of harmonic waves or wave packets as well as the distortion of solitary waves. This mathematically well-posed approach enlarges the possibility of contemporary non-destructive testing and opens new avenues of research, especially with tight connection with atomic calculations (Chen et al., 2004; Zeng et al., 2006; Maranganti and Sharma, 2007).

Finally, we hope that the detailed analysis of dispersion curves and corresponding wave profiles described in the paper could serve as a tool for the

further applications of microstructured solids under dynamical excitations.

Acknowledgement. The research over 2005 – 2012 was supported by the EU through the European Regional Development Fund, by the Estonian Ministry of Education and Research (SF 0140077s08), and by the Estonian Science Foundation (grants No. 7035, 7037, 8658, 8702).

Andrianov I.V., Awrejcewicz J., Weichert D., 2010. Improved continuous models for discrete media. Math. Probl. Engng. Article ID 986242, 35 pp.

Askes, H, Metrikine, A. V., Pichugin, A. V., Bennett, T., 2008. Four simplified gradient elasticity models for the simulation of dispersive wave propagation Phil. Mag., 88, 3415–3443.

Berezovski, A., Engelbrecht, J., Berezovski, M., 2011. Waves in microstructured solids: a unified viewpoint of modeling. Acta Mech. 220, 349–363.

Berezovski, A., Engelbrecht, J., Maugin, G. A., 2009. One-dimensional microstructure dynamics, in: Ganghoffer, J.-F., Pastrone, F. (Eds.), *Mechanics of Microstructured Solids: Cellular Materials, Fibre Reinforced Solids and Soft Tissues*. Springer, Series: Lecture Notes in Applied and Computational Mechanics, Vol. 46, pp. 21–28.

Berezovski, A. Engelbrecht, J. Maugin, G. A., 2011. Generalized thermomechanics with dual internal variables. Arch. Appl. Mech. 81, 229–240.

Berezovski, A., Engelbrecht, J., Peets, T., 2010. Multiscale modelling of microstructured solids. Mech. Res. Comm. 37, 531–534.

Born, M., von Kármán, T., 1912. Über Schwingungen in Raumgittern. Phys. Zeitschrift, 13, 297–309.

Capriz, G., 1989. *Continua with Microstructure*, Springer, Heidelberg.

Chen W. and Fish J., 2001. A dispersive model for wave propagation in periodic heterogeneous media based on homogenization with multiple spatial and temporal scales. J. Appl. Mech., Trans. ASME, 68, 153–161.

Chen, Y., Lee, J. D., Eskandarian, A., 2004. Atomistic viewpoint of the applicability of microcontinuum theories. Int. J. Solids Struct. 41, 2085–2097.

Christov, C. I., Maugin, G A., Porubov, A V., 2007. On Boussinesqs paradigm in nonlinear wave propagation. C. R. Mecanique 335, 521–535.

Engelbrecht, J., 1983. *Nonlinear Wave Processes of Deformation in Solids*, Boston, Pitman.

Engelbrecht, J., Berezovski, A., Pastrone, F., Braun, M., 2005. Waves in microstructured materials and dispersion. Phil. Mag. 85, 4127–4141.

Engelbrecht, J., Pastrone, F., Braun, M., Berezovski, A., 2006. Hierarchies of waves in nonclassical materials. in: Delsanto, P. P. (Ed.) *Universality of Nonclassical Nonlinearity: Applications to Non-Destructive Evaluations and Ultrasonics*, Springer, Berlin, p. 29–47.

Engelbrecht, J., Salupere, A., Tamm, K., 2011. Waves in microstructured solids and the Boussinesq paradigm. Wave Motion, 48, 717–726.

Eringen, A. C., Suhubi, E. S., 1964. Nonlinear theory of simple microelastic solids I & II. Int. J. Engng. Sci. 2, 189–203, 389–404.

Fish, J., Chen, W., Tang, Y., 2005. Generalized mathematical homogenization of atomistic media at finite temperatures. Int. J. Multiscale Comput. Engng. 3, 393–413

Fish, J., Fan, R., 2008. Mathematical homogenization of nonperiodic heterogeneous media subjected to large deformation transient loading. Int. J. Numer. Meth. Engng. 76, 1044–1064.

Forest, S. 2009. Micromorphic approach for gradient elasticity, viscoplasticity and damage. ASCE J. Engng. Mech. 135, 117–131.

Gonella, S., Greene, M. S., Liu, W. K. 2011. Characterization of heterogeneous solids via wave methods in computational microelasticity. J. Mech. Phys. Solids, 59, 959–974.

Huang, G. L., Sun, C. T.,2008. A higher-order continuum model for elastic media with multiphased microstructure. Mech. Adv. Mater. Struct., 15, 550–557.

Janno, J., Engelbrecht, J., 2011. *Microstructured materials: inverse problems*, Springer, Berlin.

Janno, J., Engelbrecht J., 2005. Solitary waves in nonlinear microstructured materials. J. Phys. A: Math. Gen., 38, 5159–5172.

Khusnutdinova, K. R., Samsonov, A. M., Zakharov, A. S., 2009. Nonlinear lay-

ered lattice model ans generalized solitary waves in imperfectly bonded structures. Phys. Rev. E, 79, 056606.

Maranganti, R., Sharma, P. 2007. A novel atomistic approach to determine strain-gradient elasticity constants: Tabulation and comparison for various metals, semiconductors, silica, polymers and the (Ir) relevance for nanotechnologies. J. Mech. Phys. Solids, 55, 1823–1852.

Mariano, P. M. 2008. Cracks in complex bodies: Covariance of tip balances. J. Nonlinear Sci. 18, 99–141.

Maugin, G. A., 1995. On some generalizations of Boussinesq and KdV systems. Proc. Estonian Acad. Sci. Phys. Mat. 44, 40–55.

Maugin, G. A., 2011. *Configurational Forces: Thermomechanics, Physics, Mathematics, and Numerics*, Chapman & Hall/CRC, Boca Raton, FL.

Metrikine, A. V., 2006. On causality of the gradient elasticity models. J. Sound Vibr. 297, 727–742.

Metrikine, A. V. and Askes, H., 2002. One-dimensional dynamically consistent gradient elasticity models derived from a discrete microstructure. Part 1: Generic formulation. Eur. J. Mech. A/Solids 21, 555–572.

Mindlin, R. D., 1964. Micro-structure in linear elasticity. Arch. Rat. Mech. Anal. 16, 51–78.

Papargyri-Beskou, S., Polyzos, D. and Beskos, D.E. 2009. Wave dispersion in

gradient elastic solids and structures: A unified treatment. Int. J. Solids Struct. 46, 3751–3759.

Pastrone, F., 2010. Hierarchy structures in complex solids with micro scales. Proc. Estonian Acad. Sci., 59, 79–86.

Peets, T., 2011. Dispersion analysis of wave motion in microstructured solids. Theses of Tallinn University of Technology. B, Thesis on natural and exact sciences. Tallinn: TUT Press, 121 pp.

Peets, T., Randrüüt, M., Engelbrecht, J., 2008. On modelling dispersion in microstructured solids. Wave Motion, 45, 471–480.

Porubov, A. V., 2003. *Amplification of Nonlinear Strain Waves in Solids.* World Scientific, Singapore.

Randrüüt, M., Salupere, A., Engelbrecht, J., 2009. On modelling wave motion in microstructured solids. Proc. Estonian Acad. Sci., 58, 241–246.

Randrüüt, M., Braun, M., 2010. On one-dimensional solitary waves in microstructured solids. Wave Motion, 47, 217–230.

Salupere, A., Tamm, K., Engelbrecht, J., 2008. Numerical simulation of interaction of solitary deformation waves in microstructured solids. Int. J. Non-Linear Mech. 43, 201–208.

Salupere, A., 2009. The pseudospectral method and discrete spectral analysis, in: *Applied Wave Mathematics: Selected Topics in Solids, Fluids, and Math-*

ematical Methods. Quak, E., Soomere, T., (Eds.), Springer, Heidelberg, pp. 301–333.

Santosa, F., and Symes, W. W., 1991. A dispersive effective medium for wave propagation in periodic composites. SIAM J. Appl. Math. 51, 984–1005.

Tamm, K., 2011. Wave propagation and interaction in Mindlin-type microstructured solids: numerical simulation. Theses of Tallinn University of Technology. B, Thesis on natural and exact sciences. Tallinn: TUT Press, 183 pp.

Ván, P., Berezovski, A., Engelbrecht, J., 2008. Internal variables and dynamic degrees of freedom. J. Non-Equilib. Thermodyn., 33, 235–254.

Wang, X., Lee, J. D. 2010. Micromorphic theory: a gateway to nano world. Int. J. Smart Nano Mater. 1, 115–135.

Wang, Z.-P. and Sun, C.T. 2002. Modeling micro-inertia in heterogeneous materials under dynamic loading. Wave Motion 36, 473–485.

Whitham, G. B., 1974. *Linear and Nonlinear Waves.* New York, Wiley.

Zeng, X. Chen, Y. Lee, J. D. 2006. Determining material constants in nonlocal micromorphic theory through phonon dispersion relations. Int. J. Engng Sci. 44, 1334–1345.